This Page Is Inserted by IFW Operations
and is not a part of the Official Record

BEST AVAILABLE IMAGES

Defective images within this document are accurate representations of the original documents submitted by the applicant.

Defects in the images may include (but are not limited to):

- BLACK BORDERS
- TEXT CUT OFF AT TOP, BOTTOM OR SIDES
- FADED TEXT
- ILLEGIBLE TEXT
- SKEWED/SLANTED IMAGES
- COLORED PHOTOS
- BLACK OR VERY BLACK AND WHITE DARK PHOTOS
- GRAY SCALE DOCUMENTS

IMAGES ARE BEST AVAILABLE COPY.

As rescanning documents *will not* correct images, please do not report the images to the Image Problem Mailbox.

Radiation Effects, 1979, Vol. 42, pp. 169–178
0033-7579/79/4203-0169$04.50/0

© 1979 Gordon and Breach Science Publishers, Inc.
Printed in Holland

CRYSTALLOGRAPHIC NATURE AND FORMATION MECHANISMS OF HIGHLY IRREGULAR STRUCTURE IN IMPLANTED AND ANNEALED Si LAYERS

F. F. KOMAROV, V. S. SOLOV'YEV and S. Yu. SHIRYAYEV

Institute of Applied Physical Problems, Byelorussian State University, Minsk, U.S.S.R.

(*Received January 9, 1979, in final form April 30, 1979*)

The state of the structure in (111)- and (001)-orientated Si single crystals was studied by backscattering of channelled He^+ ions, transmission electron diffraction and electron microscopy techniques after Ar^+, Si^+ and P^+ ion implantation and high temperature annealing.

The formation processes of an anomalously high residual disordering in recrystallised layers were shown to be based on the deformation twinning mechanism which is unique for all types of ions. Deformation twinning in implanted layers is induced by the internal stresses caused by the action of two factors. The first is due to the chemical nature of an impurity to be implanted, particularly, to a blistering effect in the case of Ar^+ implantation. The spatial inhomogeneity of the amorphized layer structure is responsible for the second factor. The role of specimen crystallographic orientation as well as the role of implantation temperature in recrystallization processes of implanted layers are discussed.

INTRODUCTION

Ion implantation into Si single crystals is unavoidably accompanied by the disordering of the crystalline structure and the amorphisation of the implanted layers at certain conditions. As a rule the recovery of the structure after high temperature annealing is incomplete that is due to the formation of residual defects of high concentration. Among a wide range of observed types of residual defects, highly irregular structure (HIS) formed in a number of cases are of great importance. They comprise microtwins and polycrystalline inclusions of silicon, which have been already observed.[1–3] It is the formation of HIS which, in our opinion, determines the anomalies in the behavior of the main doping impurities, introduced into Si layers after Ar^+ implantation and annealing.[4,5] Gettering properties of such layers as regards radiation defects[6] should also be associated with the peculiarities of their structure state.

The literature on the formation of HIS available at present is rather unsystematic. The HIS appearance, as a rule, is noticed as an accompanying effect in the studies performed. The most important results are basically related to the cases of Ar^+[7,8] and Si^+[9,10] ion implantation. Specifically, in Ref. (7) the authors established the identity of the character of the structure in amorphous Si layers, prepared by vacuum deposition or 50 keV Ar^+ ion implantation and recrystallized on a single-crystalline Si substrate.

In accordance with the results of Ref. (9) the HIS formation may considerably influence the recrystallization kinetics of Si layers, amorphized by ion implantation. In Ref. (11) the appearance and interpretation of microtwin reflections was discussed in some detail. In Ref. (12) the formation of twins in Si at the interface between irradiated and underlying material was reported.

At the same time the reasons and mechanisms for the formation of the anomalously high residual disordering have not yet been studied profoundly so far. The role of the chemical nature of the implanted impurity and that of the sample crystallographic orientation in the HIS formation processes is still unknown. The present paper is devoted to studying the problems mentioned above, whose solution would allow the experimental data on HIS to be systematized.

2 EXPERIMENTAL PROCEDURE

The studies were performed on (111)- and (001)-oriented single crystal Si samples after Ar^+, Si^+ and P^+ ion implantation and 30 min. annealing at 800°C in inert atmospheres. The chanelling effect

MAY 03 2004 10:25 FR CIST! ICIST 613 993 1395 TO 13123214299 P.04/11

during implantation was suppressed by disorientating the samples in respect of the ion beam at an angle of more than 7°.

Backscattering (BS) of channelled He^+ ions with energies of 1.1 and 1.4 MeV, transmission electron diffraction and transmission electron microscopy (TED, TEM) techniques under an accelerating voltage of 100 kV were used for the analysis of the state of the structure in the implanted layers. Scanning electron microscopy was also used. The procedure for taking the BS spectra is discussed in detail in Ref. (13). Thin foils with a thickness of ~ 0.2 μm intended for examinations by an electron microscope were prepared by a chemical polishing on the side opposite to the bombarded surface. Dislocation-type defects were analyzed from the electron-microscopic images using a variety of diffracting conditions ({220}, {311}, {400}).[14,15] Controlled removal of layers through anodic oxidation and etching was used for the structural analysis at large depths.

3 RESULTS

3.1 Ar^+ Ions

Implantation of Ar^+ ions with energies of 60 and 200 keV in the dose range 5×10^{13} to 5×10^{15} ions/cm^2 was performed at 20°C. Consider the case of implantation into the (111)-oriented 200 keV samples.

Figure 1a shows the He^+ ion energy spectra obtained from the samples before and after implantation when the analyzing beam was incident either along the ⟨111⟩ crystallographic direction (the axial spectra 1 to 5) or in the non-oriented direction (spectrum 6). One of the bottom scales is the depth scale allowing the BS yield to be directly estimated at different distances from the sample surface.

After implantation with the introduction of radiation damage the BS yield for the channelled beam increases due to the scattering at the defects and at a dose of 2.5×10^{14} ions/cm^2 reaches the non-oriented beam yield. This indicates the formation of an amorphous layer at a certain depth. A further dose increase results in its expansion towards the surface and deep inside the target. At a dose of 1×10^{15} ions/cm^2 a continuous amorphous layer is formed. The analysis of BS spectra for the implanted samples subjected to annealing at 800°C (Figure 1b) indicates an anomalously high residual disordering in the case when a considerable

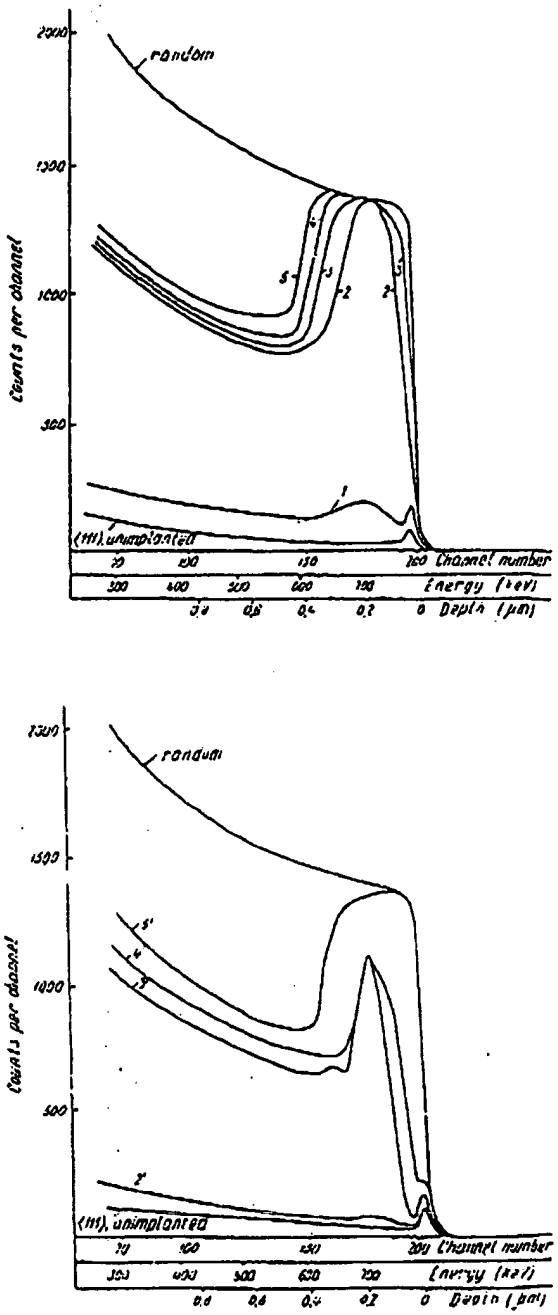

FIGURE 1 BS spectra of He^+ ions from the Si samples obtained: (a) after Ar^+ ion implantation with an energy of 200 keV. The implantation doses: (1) 5×10^{13}; (2) 2.5×10^{14}; (3) 7×10^{14}; (4) 1×10^{15}; (5) 5×10^{15} ions/cm^2; (b) after implantation and 900°C annealing for 30 min. Primes at the figures indicate an additional annealing ($E_{He^+} = 1.4$ MeV).

FIGURE 2
etched in the
ions/cm^2. 80
bubbles, reve

volume of
is highly re
after impla
ions/cm^2 a
~ 0.2 μm,
ion projec
ions/cm^2
almost one
the case o
under equ
negligibly
the implar
chemical n
for the hi
Generatio
is characte
implanted
Ar^+ ions
by scannin
conditions
$T_{anneal.} =$
face erosio
After short
shaped cra
gas bubbl
polished
effect upor
structure
samples b
ions/cm^2
the struct
single-crys
retained (
In the
the bomb

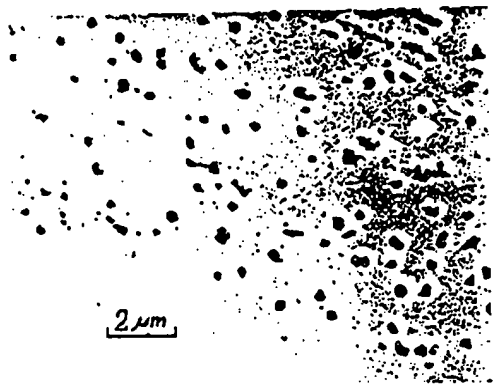

FIGURE 2 Scanning electronic micrograph of the Si surface etched in the polishing etcher. The Ar^+ ion dose is 5×10^{15} ions/cm^2, 800°C annealing for 30 min. Dark spots are gas bubbles, revealed through etching.

volume of the bombarded sample is amorphized. It is highly remarkable that the maximum disordering after implantation of doses 2.5×10^{14} to 2×10^{15} ions/cm^2 and annealing is observed at a depth of ~0.2 μm, i.e. it practically coincides with the Ar^+ ion projected range.[16] At a dose of 5×10^{15} ions/cm^2 the degree of the residual disorder is almost one order of magnitude higher than that in the case of P^+ ion implantation and annealing under equal conditions.[13] The ion masses differ negligibly and the magnitude of the damage after the implantation is almost the same. Hence, the chemical nature of Ar as an impurity is reasonable for the high residual disorder of the structure. Generation of gas bubbles under certain conditions is characteristic of the behaviour of inert gases implanted into a crystalline lattice. On implanting Ar^+ ions a blistering effect was directly observed by scanning electron microscopy in more extreme conditions ($D = 5 \times 10^{16}$ ions/cm^2, $T_{impl.} = 400$°C, $T_{anneal} = 600$°C).[17] Here the characteristic surface erosion of a blistering effect was not discovered. After short-time etching (~2 sec), however, round-shaped craters (Figure 2) representing the traces of gas bubbles appear on the surface of the slowly polished specimen. The influence of blistering effect upon the character of the recrystallized layer structure was determined by TEM technique. The samples bombarded with a dose of 1×10^{15} ions/cm^2 are the most important since in this case the structure residual damage is fairly large but single-crystalline properties are simultaneously retained (Figure 1b).

In the layers with a depth of 0 to 3000 Å from the bombarded surface inhomogeneous grained

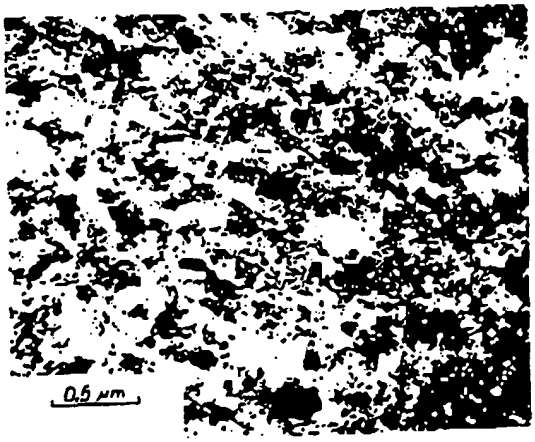

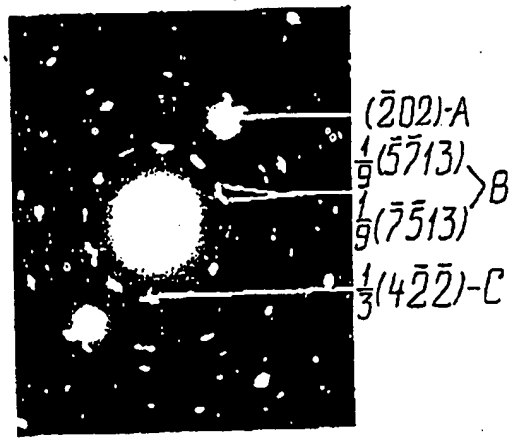

FIGURE 3 Transmission electron micrographs (a) and TED-pattern (b) for the (111)-orientated Si samples bombarded with Ar^+ ions (1×10^{15} ions/cm^2, 200 keV) after 800°C annealing for 30 min (A is the matrix reflection, B is reflection caused by second-order twinning, C is a reflection of a double positioning).

contrast (Figure 3a) is observed. The TED pattern from these layers (Figure 3b) exhibits an intensive net of irrational spots (extra-reflections) along with the diffraction pattern from the (111)-orientated single-crystalline Si. The presence of streaks and the lack of any signs of Kikuchi-pattern is also typical confirming a high degree of the residual disordering.

In accordance with the analysis, performed in Ref. (7), the set of extra-reflections observed can be separated into two groups (Figure 5):

1) Extra-reflections caused by a second-order twinning in all possible {$\bar{1}$11}-planes inclined to the sample surface. The model of a second-order

MAY 03 2004 10:25 FR CISTI ICIST 613 993 1395 TO 13123214299 P.06/11

twinned structure suggests that the secondary twins are arranged both at "downward-pointing" and "upward-pointing" {111} faces of the primary twins in the Ino hexagonal model†.[18] The matrix of this structure has one of the {111}-planes parallel to the sample surface.

2) Extra-reflections caused by the diffraction at the boundaries of a double "positioning".[19] The double positioning boundaries result from the twinning along the (111)-planes parallel to the sample surface.

The twin material distribution was studied by the dark-field patterns formed within the matrix and twin reflections. Together with the TED data this allowed the grained contrast observed to be identified as the aggregates of the first- and second-order microtwin plates, lying in all possible {111}-planes. The aggregates under consideration have no strict crystallographic faces. A certain disorientation from the real position of the microtwin blocks which is manifested in the TED-patterns as the radial lengthening of reflections (Figure 3b) and the presence of a low concentration of the polycrystalline material should be noted.

The layers lying immediately behind the region of the maximum residual disordering (at a depth of 3000 to 5000 Å) have a more perfect structure. This is indicated by the appearance of Kikuchi-patterns and the the absence of any additional reflections in the electron diffraction patterns. The TEM investigations have shown that only perfect dislocation loops of irregular form with a size of 1000 to 3000 Å mainly of interstitial type are observed at depth in question.

In the case of 60-keV Ar^+ ion implantation, (001)-orientated samples were also used. The (111)-orientation results coincide basically with those obtained for the 200 keV energy, i.e. after 800°C annealing of the samples, implanted with a dose of 10^{15} ions/cm^2, a second-order twinning is observed in the bombarded layers. Microtwin layer conjugates with the matrix through a layer of dislocation loops of irregular form. The processes under consideration are developed at a considerably lower depth from the bombarded surface which is naturally associated with the implantation energy decrease. Annealing of the

(a)

(b)

FIGURE 4 Transmission electron micrograph (a) and TED-pattern (b) for the (001)-orientated Si samples bombarded with Ar^+ ions (5×10^{15} ions/cm^2, 60 keV) after 800°C annealing for 30 min.

(001)-orientated samples, implanted with a dose of 1×10^{15} ions/cm^2 does not result in the HIS formation. A high density of the interstitial-type dislocation loops is observed. Microtwinning appears at a dose of 5×10^{15} ions/cm^2. At least second-order twinning is observed in this case as in the case of the (111)-orientation, which is confirmed by the TED-pattern (Figure 4b). The twin material density is considerably lower than that in the case of the (111)-oriented samples. This allows the interstitial dislocation loops to be

† Under second-order twinning the relation between the twin and the matrix rather than those between the twins themselves is meant.[20]

simultaneously ordered layers a (Figure 4a).

3.2 Si^+ Ions

Implantation o 20°C into the (the dose rang ions/cm^2.

The BS spec damage accum ion dose rise. damage takes a peak in the B dose, while its w until amorphis of crystal is a layer expansio that in the c observed.

Along with t peak is formed parable to tha however, the while the sur value and merg separation of detector limit r of the 192 to tinguished. Th dose variatio 3.8×10^{14} ion

It should be kinetics and layers, corresp gous for the (sample. At the implanted wit the (111) case results in the disorder consi spatial inhom trum for the with a dose o is observed sli initial sample.

The charac the (111)-orie previous cases layers. This obtained fro

MAY 03 2004 10:25 FR CISTI ICIST 613 993 1395 TO 13123214299 P.07/11

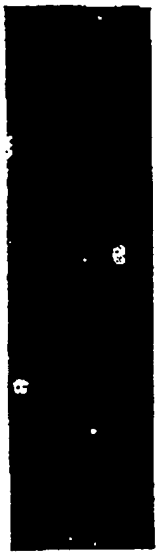

aph (a) and TED-
s bombarded with
· 800°C annealing

d with a dose
ult in the HIS
ie interstitial-
Microtwinning
/cm². At least
in this case as
which is con-
4b). The twin
wer than that
samples. This
loops to be

simultaneously resolved both in the highly disordered layers and in the layers lying behind them (Figure 4a).

3.2 Si^+ Ions

Implantation of 60 keV Si^+ ions was performed at 20°C into the (111)- and (001)-oriented samples in the dose range from 9.6×10^{13} to 2.4×10^{16} ions/cm².

The BS spectra in Figure 5a show the radiation damage accumulation kinetics with the implanted ion dose rise. It is evident that the main part of damage takes place at a certain depth, forming a peak in the BS spectra. The peak height rises with dose, while its width remains practically unchanged until amorphisation in the corresponding region of crystal is attained. Later on the amorphous layer expansion occurs, i.e. the same situation as that in the case of argon ion implantation is observed.

Along with the principle damage peak the surface peak is formed. At a low dose its height is comparable to that of the principle peak. Later on, however, the principle peak grows more rapidly while the surface peak achieves its saturation value and merges with the principle one. Although separation of the both peaks is limited by the detector limit resolution, nevertheless in the region of the 192 to 194 channels a step can be still distinguished. The step height changes negligibly with dose variation in the interval 2.4×10^{14} to 3.8×10^{14} ions/cm².

It should be noted that the defect accumulation kinetics and the thicknesses of the amorphous layers, corresponding to identical doses, are analogous for the (111)- and (001)-orientations of the sample. At the same time annealing of the samples implanted with a dose of 2.8×10^{15} ions/cm² in the (111) case as compared to the (001)-orientation results in the formation of the lattice residual disorder considerably higher by magnitude and spatial inhomogeneity (Figure 5b). The BS spectrum for the (001)-oriented Si sample implanted with a dose of 2.4×10^{15} ions/cm² and annealed is observed slightly above the spectrum from the initial sample.

The character of this large residual damage for the (111)-oriented samples is caused as in the previous cases, by the twinning in the near-surface layers. This is confirmed by the TED-pattern obtained from the Si samples implanted with a

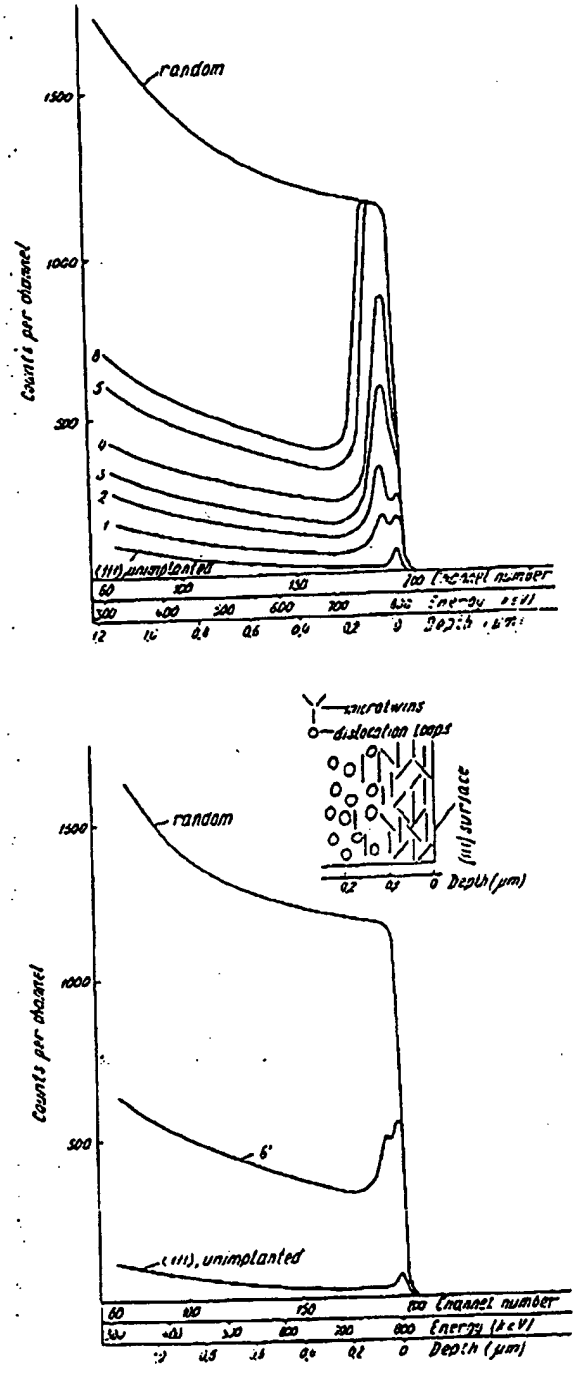

FIGURE 5 BS spectra of He^+ ions from the (111)-orientated Si samples obtained: (a) after Si^+ ion implantation with an energy of 60 keV. Implantation doses: (1) 9.6×10^{13}; (2) 1.9×10^{14}; (3) 2.4×10^{14}; (4) 3.8×10^{14}; (5) 7.2×10^{14}; (6) 2.4×10^{15} ions/cm²; (b) after implantation and 800°C annealing for 30 min. The diagram of the depth distribution for the types of defects is also presented (E_{He^+} = 1.4 MeV).

dose of 2.4×10^{15} ions/cm^2 and annealed (Figure 7b). The TED-pattern under consideration essentially differs from those observed previously (Ar^+ ions) by the lack of the extra-reflections caused by the second-order microtwins. This indicates a predominantly simple first-order twinning in the recrystallized layers. At depths corresponding to the decay at the defect profile (~800 Å; Figure 5b) the microtwin density rapidly falls down with the removal from the sample surface. It is typical that the rate of their density decrease with increasing depth is considerably higher for microtwins lying in the {$\bar{1}$11}-planes inclined to the sample surface. This results in that at depths above 1200 Å along with the high concentration of interstitial loops of irregular form only the sample-surface parallel microtwins are observed. Their density continues to fall down with the increasing depth. At a depth of about 1800 Å only dislocation loops are observed. The diagram of the defect type depth distribution is presented in Figure 5b together with the BS spectra.

A considerably lower residual damage in the case of the (001)-oriented samples is related to the presence of the highly concentrated dislocation loops in the recrystallized layers. Both complete and partial hexagonal Frank loops, lying in all possible {111}-planes are observed. The analysis of the loop nature indicates that all of them are of the interstitial type.

3.3 P^+ Ions

Implantation of P^+ ions was perfomed into the (111)-oriented Si samples with energies of 35 and 200 keV. The implantation temperatures at an energy of 35 keV was 20°C and that at an energy of 200 keV was −196°, 20° and 200°C.

The BS spectra presented in Figure 6a indicate temperature dependence of the depth disorder of the Si single-crystals bombarded with P^+ ions to a dose of 5×10^{15} ions/cm^2. The formation of amorphous layers near the sample surface occurs at implantation temperatures of −196° and 20°C. At 200°C a considerably lower disordering of the sample crystalline structure is insufficient for its amorphisation to be observed. The main effect of implantation temperature upon the character and magnitude of the primary disorder is clearly revealed after annealing of the implanted samples. The maximum residual disorder is observed at an implantation temperature of −196° and concentrated within a thin layer (as compared to the

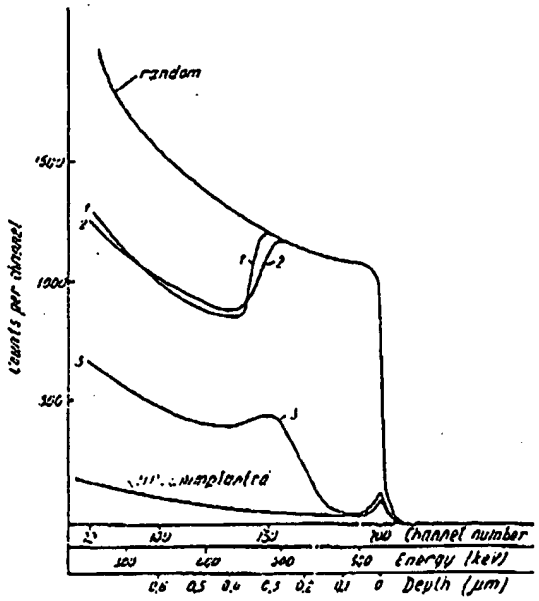

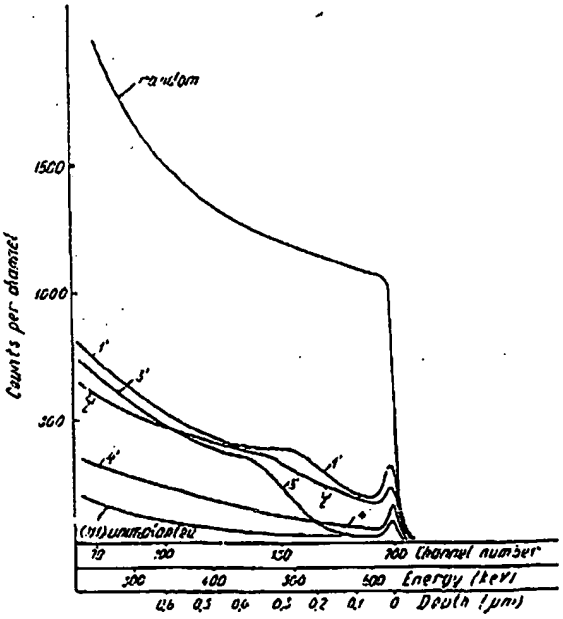

FIGURE 6 BS spectra of He^+ ions from the (111)-oriented Si samples obtained: (a) after P^+ ion implantation (1×10^{15} ions/cm^2, 200 keV). The implantation temperatures: (1) −196°C; (2) 20°C; (3) 200°C. Spectrum 4 corresponds to the implantation at 35 keV with 1×10^{15} ions/cm^2 at 20°C; (b) after implantation and 800°C annealing for 30 min. (E_{He^+} = 1.1 MeV).

FIGURE 7
(111)-orient
with 1 × 10
30 min; (b)
HIS for the

amorphou
sample s
implantat
decrease
residual d
defects lo
cally coinc
Annealing
tion of the

MAY 03 2004 10:26 FR CISTI ICIST 613 993 1395 TO 13123214299 P.09/11

(a)

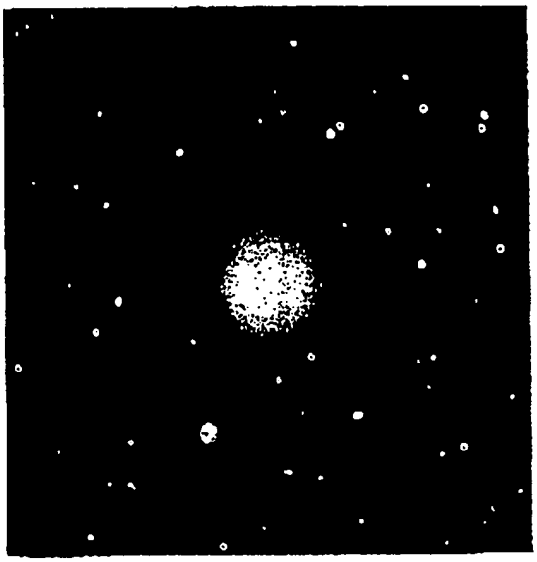

(b)

FIGURE 7 Transmission electron micrograph (a) for the (111)-orientated Si samples bombarded with P^+ ions at 200 keV with 1×10^{15} ions/cm^2 at 20°C, and annealed at 800°C for 30 min; (b) typical TED-pattern from the samples containing HIS for the cases of Si^+ and P^+ ion implantation.

amorphous layer) lying immediately near the sample surface (Figure 6b). The increase in implantation temperature up to 20°C results in the decrease both of the height and width of the residual disorder peak. At 200°C the peak of the defects localized near the sample surface practically coincides with the original single-crystal peak. Annealing of the samples, amorphized by implantation of the 35-keV P^+ ions at 20°C also leads to the formation of a negligible residual disorder (spectrum 4, Figure 6b).

The studies performed by TEM technique show that a small residual disorder in the cases of implantation of $^+$ ions with an energy of 200 keV at 200°C and with an energy of 35 keV at 20°C is due to the presence of highly-concentrated dislocation loops near the sample surface.

The increase in the BS yield for implantation temperatures of −196°C and 20°C is associated with the formation of microtwins near the sample surface. Primary microtwins as indicated by the TED-patterns in Figure 7b are mainly similar to those seen in the case of Si^+ ion implantation. At the same time the lowest degree (as compared to the HIS considered above) of the recrystallized layer structure splitting is observed. Individual large microtwin lamellae, lying in the extended matrix regions, are well resolved in the TEM-pattern (Figure 7a). As previously, at a certain depth the microtwin density begins to decrease and at a depth exceeding the range of the surface peak the interstitial dislocation loops become the dominant type of defects.

4 DISCUSSION AND CONCLUSION

The analysis of the above results indicates that two factors considerably influence the magnitude of the residual disorder in the recrystallized layers. On the one hand it is the chemical nature of the implanted impurity. On the other hand it is the inhomogeneity of the radiation damage spatial distribution.

The results on Ar^+ ion implantation serve as a strong evidence to the first. The blistering effect caused by the inertness of the impurity to be implanted is responsible for the intense microtwinning in the recrystallized layers in this case. The bubble nuclei seem to be already formed during implantation. Polyvacancy clusters–V–V–centers[21] may be, for instance, nucleation centers. Upon annealing the nuclei are growing due to Ar atoms migrating towards them. Recrystallization of the gas bubbles is accompanied by the increase in their internal pressure which leads to the onset of strong local internal stresses. The latter on reaching some critical value induces plastic deformation of recrystallising layer microvolumes in the multiple twinning mechanism. The high value and locality

of the internal stresses fields determine both a small size of the microtwins and a stronger splitting of the structure. It should be mentioned that the chemical nature factor in the case of HIS formation can be produced not only by the blistering effect. The onset of the internal stresses during recrystallization may be caused by the precipitation of the second phase particles, for instance, SiO_x, SiC, Si_xN_y,[22] in the case of O^+, C^+, N^+ ion implantation. A large concentration of impurities may also be contained in the vacuum-deposited amorphous Si layers originating from the residual gases in the vacuum systems.[23] Annealing of such layers at temperatures above 900°C results in the formation of a noticeable concentration of the SiC-phase. Therefore it is not surprising that in the recrystallized Si layers, obtained by Ar^+ ion implantation and vacuum deposition, identical multiply twinned structures are formed as it was observed in Ref. (7). HIS formation seems to be also expected upon precipitation of slightly soluble impurity particles, as pointed out in Ref. (24) in the case of Sb^+ ion implantation.

A somewhat different situation arises upon Si^+ ion implantation since the influence of the chemical nature of the implanted impurity is excluded. The similarity of many crystallographic peculiarities of HIS for all types of ions under consideration indicates that in this case as well the origin of microtwinning should be looked for in the internal stresses.

The BS spectra for Ar^+- and Si^+-ion implanted samples (Figure 1a, 5a) indicate a strong spatial inhomogeneity of the structure disorder. In the first approximation it is associated with the inhomogeneous distribution of specific elastic energy loss of ions. Another important feature is the defect migration from the maximum elastic energy loss region as well as their annealing during implantation. From this viewpoint the formation of the surface defect peak together with the inner one can be well explained, as being established earlier for light ions.[25] A stimulating influence upon the migration processes is produced by the proximity of the surface and by the excitation and ionisation effects in the near surface region.[26]

The inhomogeneity of the radiation damage spatial distribution should be responsible for the spatial inhomogeneity of the amorphous layer. This fact in the absence of the chemical nature factor determines the anomalies of the structure state in the recrystallized layers. The inhomogeneity in character of the disorder in the amorphous layers produces the inhomogeneous internal stresses parallel to the sample surface. Their relaxation is achieved through twinning in the recrystallized layers. It should be mentioned that normal components caused by the swelling of the amorphous layer should also exist in the system of the internal stresses. At the same time it is the tangential stresses which basically dominate the recrystallization character. This is confirmed by the anistropy of the HIS formation effect. The lack of twinning if the (001)-oriented crystals under identical conditions of implantation and annealing is due to the lack of the (111)-plane of readily achieved twinning parallel to the sample surface. Thus, relaxation of the tangential constituents of the internal stresses by means of twinning is considerably cumbersome.

In the case of Ar^+ ion implantation the effect of the inhomogeneity is not excluded (especially in the case of the 200-keV implantation) as well. A considerably higher degree of the structure splitting, however, indicates that the factor of the chemical nature is dominant. The anistropy effect discovered in this case as well indicates an important role of orientation of the {111}-plane system of twinning about the sample surface in the amorphous layer recrystallization processes.

While studying the P^+ ion implantation results the following should be taken into account. The HIS formation in the case of the 200-keV implantation is due to the inhomogeneity of the structure disorder since phosphorus is a doping impurity readily soluble in Si. Twinning is not observed at a low (35 keV) ion energy. This is associated with the formation of the defect layer immediately near surface, that considerably cuts down the inhomogeneity of the structure spatial disorder. A temperature rise during implantation can eliminate the effects of HIS formation during annealing. The latter is primarily due to that the implanted layers were not amorphized.

On the other hand, upon phosphorus atom incorporation into interstitial sites during annealing, incomplete relaxation of comprehensive stresses, since the tetrahedral covalent radius for phosphorus atoms is smaller than that for silicon atoms. This fact can, to some extent, account for the stimulating effect of the implanted phosphorus on the epitaxial recrystallization processes, observed in Ref. (27), as well as the lowest degree of the material crushing when microtwinning takes place in our experiments of phosphorus ion implantation.

REFERENCES

1. S. M. Davi 19 (1970).
2. D. J. Maze 17, 1145 (1
3. L. N. Lar 589 (1967).
4. V. T. Karm and A. F. K
5. V. T. Karm Zorin, *Fiz.*
6. Murase Ka 4404 (1977)
7. Iwao Ohdo (1977).
8. D. Baither *Implantatio*
9. L. Csepreg *Lett.*, 29, 9.
10. G. H. Sch L. F. Lowe.
11. M. D. Ma (1969).
12. D. J. Maze *Reg. Conf.*
13. G. Götz. I *Exper. Tec*
14. P. B. Hirsh and M. J. *Thin Cryst*

REFERENCES

1. S. M. Davidson, *Proc. European Conf. on Ion Implantation*, 19 (1970).
2. D. J. Mazey, R. S. Nelson, and R. S. Barnes, *Phil. Mag.*, 17, 1145 (1968).
3. L. N. Large and R. W. Bicknell, *Journ. Mater. Sci.*, 2, 589 (1967).
4. V. T. Karmanov, P. V. Pavlov, E. I. Zorin, D. I. Tetelbaum and A. F. Knokhlov, *Fiz. Tekh. Poluprov.*, 9, 1786 (1975).
5. V. T. Karmanov, A. F. Khokhlov, P. V. Pavlov, and E. I. Zorin, *Fiz. Tekh. Poluprov.*, 11, 1871 (1977).
6. Murase Katsumi and Harada Hivoyuki, *J. Appl. Phys.*, 48, 4404 (1977).
7. Iwao Ohdomari and Nobuyki Onoda, *Phil. Mag.*, 35, 1373 (1977).
8. D. Barther and J. Krylov, *International Conference on Ion Implantation in Semiconductors*, Budapest, 155 (1975).
9. L. Csepregi, J. W. Mayer, and T. W. Sigmon, *Appl. Phys. Lett.*, 29, 92 (1976).
10. G. H. Schwuttke, K. Brack, E. F. Gorey, A. Kahan, L. F. Lowe, and F. Euler, *Phys. Stat. Sol. (a)*, 14, 107 (1972).
11. M. D. Matthews and P. F. James, *Phil. Mag.*, 19, 1179 (1969).
12. D. J. Mazey, R. S. Nelson and R. S. Barnes, *Proc. 4th Eur. Reg. Conf. on Electron Microscopy*, Rome, 367 (1968).
13. G. Götz, K.-D. Klinge, F. Shwabe, and V. Solov'yev, *Exper. Techn. Phys.*, 25, 71 (1977).
14. P. B. Hirsh, A. Howie, R. B. Nicholson, D. W. Pashley, and M. J. Whelan, *Transmission Electron Microscopy of Thin Crystals* (Butterworths, London, 1965).
15. V. M. Kosevich and L. S. Palatnik, *Elektronnomikroskopicheskie izobrazheniya dislokatsii i defektov upakovki* ("Nayka," Moscow, 1976).
16. M. A. Kumakhov, V. A. Muralev, E. G. Aver'yanov, V. A. Smirnov, and A. P. Khavkin, Proyektivnye probegi i razbrosy probegov dlya 1240 kombinatsii ion-mishen' v intervale energii 20keV E 1000 keV, Moscow, Vsesoyuzn. Vsesoyuzn. instit. nauchn. i tekhnich. inform. dep. No. 700–75.
17. G. Götz, E. Glaser, F. Shwabe, Trudy VI Vsesoyuznogo soveshchaniya po fizike vzaimodeistviya zaryazhennykh chastitz s monokristallami, Moscow, 513 (1975).
18. S. Ino, *J. Phys. Soc. Japan*, 21, 346 (1966).
19. D. W. Pashley and M. J. Stowell, *Phil. Mag.*, 8, 1605 (1963).
20. J. A. Kohn, *Amer. Mineralogist*, 43, 263 (1958).
21. N. N. Gerasimenko, A. V. Dvureshenskii, and L. S. Smirnov, *Fiz. Tekh. Poluprov.*, 5, 1700 (1975).
22. P. V. Pavlov, T. A. Kruse, D. I. Tetelbaum, E. I. Zorin, E. V. Shitova and N. V. Gudkova, *Phys. Stat. Sol. (a)* 36, 81 (1976).
23. E. G. Kostin, *Fiz. elektron. Respublik. mezhved. nauchn. tekhn. sborn.* vyp. 13, 101 (1976).
24. M. D. Matthews, *Rad. Eff.*, 11, 167 (1971).
25. S. I. Romanov and A. S. Smirnov, *Fiz. Tekh. Poluprov.*, 6, 1931 (1977).
26. J. C. Bourgoin, J. W. Corbett, and H. L. Prish, *J. Chem. Phys.*, 59, 4042 (1973).
27. L. Csepregi, J. W. Mayer, E. F. Kennedy, and T. W. Sigmon, *J. Appl. Phys.*, 48, 4234 (1977).